Enhanced Protection Scheme for Smart Grids Using Power Line Communications Techniques—Part II: Location of High Impedance Fault Position

Apostolos N. Milioudis, *Student Member, IEEE*, Georgios T. Andreou, *Member, IEEE*, and Dimitrios P. Labridis, *Senior Member, IEEE*

***Abstract*—An effective protection scheme against high impedance faults (HIFs) has to efficiently confront the issues of detection and location simultaneously. In Part I of this study the issue of detection is investigated, while in Part II a method that deals with the exact location of HIF position using an installed power line communication (PLC) system is elaborated. This method comprises specific test signal injections into the power grid after a HIF alarm is set. Using impulse responses that are recorded by the PLC devices, the location of the fault may be derived. A flowchart that describes the usage of the complete method for HIF detection and location is presented. The impulse responses that correspond to several fault cases are shown and the methodology that may lead to the fault location is explained. The effect of the fault type and its impedance on the efficacy of the method is highlighted. Finally, the model is applied to a line that is part of the Greek rural distribution system and its validity is tested.**

***Index Terms*—High impedance fault detection, power distribution faults, power line communications, power system protection, smart grids.**

I. Introduction

HIGH impedance fault detection is a challenging issue due to the nature of this kind of faults. They cannot be easily perceived because the small rise that they provoke to the system's current may also be attributed to a change to the feeder's load.

Important research has been conducted aiming to achieve HIF detection using several different methodologies which lead to an alarm set once specific criteria are met. This alarm indicates that a HIF is present along the protected transmission line's length, but is incapable of providing its actual location. The knowledge of the fault's location is of high importance, because its presence threatens the public safety. Furthermore, if a HIF alarm causes the opening of the feeder's circuit breaker for the clearance of the fault, and the HIF has to be located by a mobile utility's crew, the long time period for which several customers will be out of service inflicts the utility's reliability and causes economical damage.

For these reasons, the HIF location is a very important issue that has to be resolved. Models concerning an unsynchronized fault location scheme [1], wavelet transform [2], [3] or focusing on the location of such faults on distributed generation cases [4] have been developed. However, the very promising upgrade of the traditional power networks to smart grids may enhance their protection [5], utilizing self fault isolation [6] and network reconfiguration [7], and creates a new field of opportunities for new techniques to be evolved. Indispensable information for the function of a smart grid have to be transmitted, and several technologies are candidates for that, with power line communications (PLC) being one among them [8]. Furthermore, multi-functional systems, such the one proposed, that can operate performing distinct tasks at the same time are encouraged.

Studies have investigated the potential utilization of PLC systems for broadband data transmission on rural power distribution networks [9]–[13]. In this work, the utilization of such a system for the exact HIF location is proposed. The position at which a HIF occurs at a transmission line with an installed PLC system will be among two communication devices that are designed to transmit specific information. These two particular devices could be used for the detection of the fault, which will change the arrangement's topology. The proposed methodology exploits the PLC devices and the traveling wave phenomena [14], [15] on a transmission line once a HIF alarm is set, thus it can be easily combined with any other HIF detection technique, such as the method proposed in Part I of the companion paper. The fault location is extracted by an impulse response procedure in which once a HIF is declared, PLC devices inject a test impulse into the network. Through the comparison of the impulse response under normal operational conditions as well as when a HIF is present, the fault position may be calculated from the additional peaks that the multipath propagation, hence the reflection and transmission coefficients at the HIF point, generate to the impulse response. The utilization of this comparison, which leads to the location of the fault, ensures that the proposed method can be implemented in smart grids, which could contain high distributed generation penetration and be comprised of meshed grids [16]–[23].

Some features of an installed PLC system and its essential characteristic that may be used for HIF location are elaborated in the next section. Furthermore, a flowchart that describes the combination of the proposed HIF detection method of Part I and

Manuscript received July 14, 2011; revised October 12, 2011, February 13, 2012, and May 09, 2012; accepted July 04, 2012. Date of publication September 07, 2012; date of current version December 28, 2012. This work was supported in part by the Greek State Scholarships Foundation (SSF). Paper no. TSG-00246-2011.

The authors are with the Department of Electrical and Computer Engineering, Aristotle University of Thessaloniki, 54124 Thessaloniki, Greece (e-mail: amilioud@auth.gr; gandreou@auth.gr; labridis@auth.gr).

Digital Object Identifier 10.1109/TSG.2012.2208988

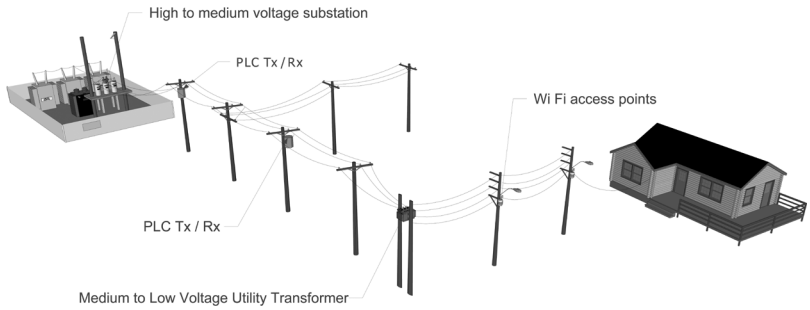

Fig. 1. Power line communications system configuration.

the model for the exact location calculation is shown in Section III. Afterwards, the method for the impulse response calculation through a recursive model for transfer function derivation [24] is described and the method is applied on different HIF cases, where its validity detecting the fault location is confirmed. Finally, in Section VI a combination of the methods that are proposed in the two parts of this work is implemented for a real rural medium voltage topology of the Greek distribution network, and significant conclusions for their efficacy are derived.

II. Features of a Power Line Communication System

The main characteristic of a PLC system is that it uses the power grid for communication purposes. Its main advantage lies to the fact that no extra wiring is needed, because the electrical wires, which transfer the electric power, are employed for the formation of the communication channel. Thus, it takes advantage of the fact that the electrical power networks extend in vast areas accommodating the majority of households. As a result, no additional investment has to be done because the network's infrastructure is already built, hence this technology has a significant benefit over other competitors.

On the other hand, electrical power distribution lines were installed for electric energy transmission purposes and not to be utilized as communication channels. As a result, electrical networks can be characterized as a hostile environment for data exchange. The existence of numerous branches creates a multipath propagation effect, similar to this of wireless communications causing, thus, significant attenuation. Nevertheless, several studies [9], [12], [13] have indicated that broadband communication via a PLC system in overhead medium voltage distribution lines is feasible, implementing a repeater span distance of 1 km.

Such an implemented system is described in general by Fig. 1, where PLC devices are installed along the distribution line's length, transmitting and receiving information, which may be either important information for the function of smart grid applications, or used for providing internet access. The data are transferred to the medium voltage level through appropriately designed coupling devices. Transformers behave as ideal filters, thus as open circuits, for the high frequencies used by PLC devices, i.e., 1–30 MHz, and bypass cables or wireless access points could be created for the successful data propagation. Thus, PLC could coexist in hybrid systems with wireless communications. A complete installed PLC system could be helpful for smart grid applications such as self healing, network restoration, smart meter functionality and in general for the transmission of data required by smart grid techniques. Moreover, this system could be used for the exact location of HIF. The key feature that can be exploited within this context involves the installation of PLC modems along the entire's line length which have high sensitivity, because they operate transmitting and receiving signals of small power spectral density (PSD). Hence, the PLC signals are characterized by small magnitudes. A pulse that is reflected at a point where a HIF occurred would have such a small magnitude as it is explained in one of the next sections, so PLC devices would be able to detect this small deviation to the measured voltage. This leads to the proposed method that utilizes installed PLC devices and implements test signals injected by them for the location of the fault. The continuous application of this test signal procedure would be impractical because the data transfer is stopped. Thus, it is important to combine this procedure with a HIF detection technique, such as the method proposed in Part I of the companion paper, which can provide a simple alarm in the case of HIF occurrence.

III. Complete Method for HIF Detection and Location

The installation of a power line communication system across a rural power distribution line may offer added functionality in addition to the transmission of information. Moreover, the topology of medium voltage lines can be regarded as static cause to the fact that the changes are rare and the utilities tend to avoid them. This fact improves the potential use of this network for data transmission and protection purposes simultaneously.

In Part I of this particular study a method was presented involving measured input impedance of a distribution transmission line utilizing the frequency range 3–95 kHz, for the detection of HIFs, as the presence of such kind of faults may significantly alter the input impedance of the arrangement at the chosen frequencies. However, only the occurrence of a fault can be recognized with this method by setting an alarm, while its specific location cannot be extracted. Therefore, an additional procedure has to be added to the proposed method for the exact location detection to be possible.

For that reason, the PLC communication devices can be utilized injecting predetermined test signals in the network. Measuring the response of the channel to these test signals the position of the fault may be determined, because its presence across a distribution line adds a discontinuity to the line's characteristic

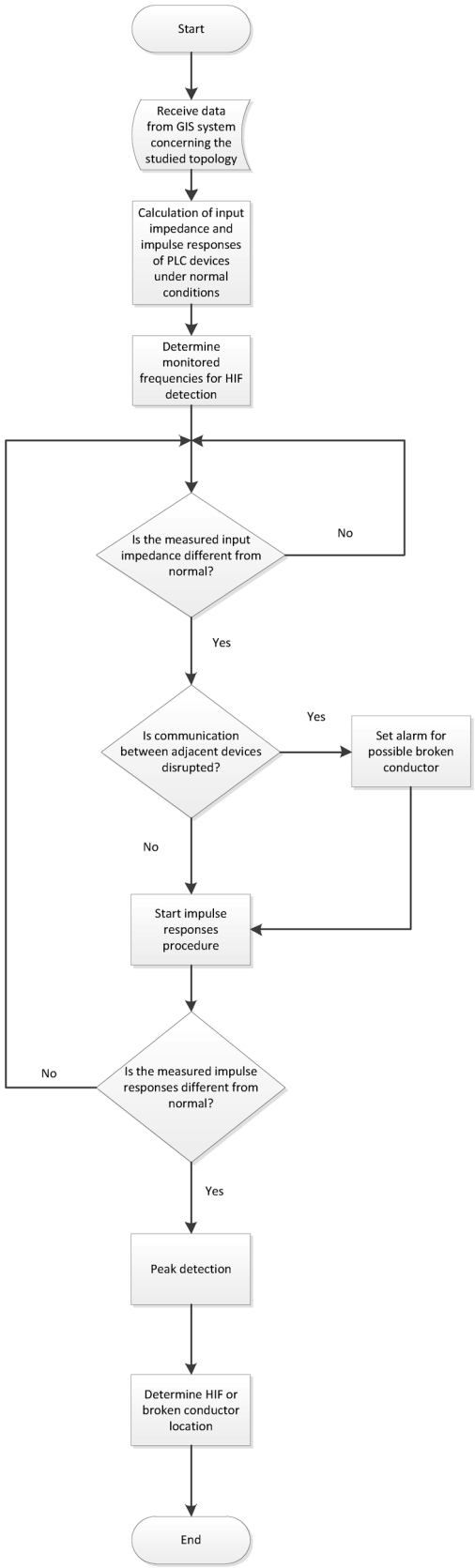

Fig. 2. Complete HIF detection and location method flowchart.

impedance, and thus, an extra point of reflection for the electromagnetic waves between two communication devices. This extra point creates distinct peaks into the channel's impulse response time sequence, and combining this information with the known propagation speed, the exact fault location is revealed.

The broken conductor case which poses the greatest danger for the public, needs a slightly different approach. The presence of a broken conductor will affect the topology's overall input impedance, as well as disrupt the communication between two adjacent devices. Therefore, a respective alarm can easily be set for the quickest possible confrontation of the problem.

A flowchart that explains the proposed method is shown in Fig. 2. The first step of the implementation requires the knowledge of the necessary information concerning the studied topology through a graphical information system (GIS). Such information would involve the branch lengths, type of conductors, geometrical arrangement, and the location of the communication devices across the transmission line. This information may be used for the calculation of the arrangement's normal input impedance and impulse responses at the points where the communication devices are installed. Using the method elaborated in Part I, specific frequencies, which perform adequately, can be determined for the monitoring of the arrangement's overall input impedance. No fault is supposed to exist while no alteration is recorded to the measured input impedance. On the contrary, if the measured input impedance is different from its normal value, an indication that a high impedance fault or a broken conductor exists is provided. For the quickest possible system restoration a check concerning the possible communication disruption between adjacent communication devices is needed. This case may correspond to a broken conductor, a communication device malfunction, as well as service interruption in the line by the power utility. The most critical among these situations is the broken conductor, as it poses danger for the public. Therefore, an alarm for a possible broken conductor is set, which however does not affect the rest of the procedure. Next, the impulse response procedure initiates, in which all the installed communication devices inject a test impulse in the network. However, the communication devices cannot be allowed to send the impulses simultaneously, as this will cause a confusion concerning the signal received by each one. Therefore, the impulse transmissions have to be time discrete. The sequence with which the devices will transmit will have to be determined by the utility. The device that produces the impulse measures the voltage pulses that return back to it and the same measurement is also held by the adjacent device. Subsequently, by comparing the measured impulse responses with those that correspond to normal operational conditions and by applying a peak detection algorithm the exact location of the fault can be calculated. Finally, possible solutions are:

- network reconfiguration, if possible for the isolation of the line's part that contains the fault; or
- the notification about the situation of a utility's crew that is responsible to repair the problem.

IV. Multipath Propagation Over Power Lines

The medium voltage distribution network is comprised of numerous line segments, branches and terminations. This results

TABLE I
MULTIPATH PROPAGATION

Path i	Routing of signal	Transfer Function of path i	Path's length d_i
1	$2 \to 6 \to 9 \to 13$	$\tau_{62} \cdot \tau_{96} \cdot \tau_{13,9} e^{-\gamma(f) \cdot d_i}$	$l_2 + l_6 + l_9 + l_{13}$
2	$2 \to 3 \to 4 \to 6 \to 9 \to 13$	$\tau_{32} \cdot \rho_{43} \cdot \tau_{64} \cdot \tau_{96} \cdot \tau_{13,9} e^{-\gamma(f) \cdot d_2}$	$l_2 + l_3 + l_4 + l_6 + l_9 + l_{13}$
3	$2 \to 3 \to 4 \to 3 \to 4 \to 6 \to 9 \to 13$	$\tau_{32} \cdot \rho_{43}^2 \cdot \rho_{34} \cdot \tau_{64} \cdot \tau_{96} \cdot \tau_{13,9} e^{-\gamma(f) \cdot d_3}$	$l_2 + 2 \cdot l_3 + 2 \cdot l_4 + l_6 + l_9 + l_{13}$
4	$2 \to 6 \to 5 \to 6 \to 9 \to 13$	$\tau_{62} \cdot \rho_{56} \cdot \rho_{65} \cdot \tau_{96} \cdot \tau_{13,9} \cdot e^{-\gamma(f) \cdot d_4}$	$l_2 + l_6 + l_5 + l_6 + l_9 + l_{13}$
5	$2 \to 6 \to 7 \to 8 \to 9 \to 13$	$\tau_{62} \cdot \tau_{76} \cdot \rho_{87} \cdot \tau_{98} \cdot \tau_{13,9} \cdot e^{-\gamma(f) \cdot d_5}$	$l_2 + l_6 + l_7 + l_8 + l_9 + l_{13}$
$\vdots$	$\vdots$	$\vdots$	$\vdots$

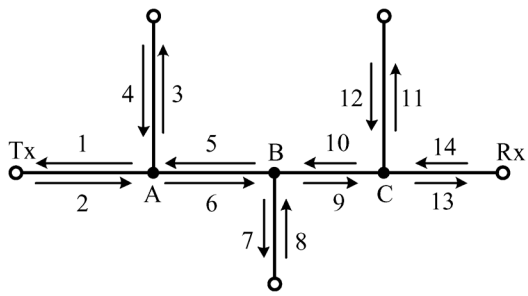

Fig. 3. Multibranched topology between two communication devices Tx and Rx having 3 junction points A, B, C.

to the formulation of a multipath propagation environment similar to a wireless communication channel, cause to the fact that a signal is subjected to reflections and transmissions at every point of discontinuity in the characteristic impedance, as well as at the points where the transmission line is terminated to an impedance different from the characteristic one. Therefore, every signal that propagates from a transmitting device towards a receiving one over the distribution network, reaches its destination in a form of several replicas that arrive at different time delays according to the several propagation paths that exist between them.

A part of a distribution network located between a transmitting (Tx) and a receiving device (Rx) that contains 14 numbered directional segments is shown in Fig. 3. Generally, the transfer function between two points in this topology is given by (1)

$$H(f) = \sum_{i=1}^{P} g_i \cdot e^{-\gamma(f) d_i} \tag{1}$$

where i is the path that the signal follows. Theoretically an infinite number P of paths exist, but in practice only a specific number of P_s significant paths have to be taken into account. Furthermore, g_i is a weighting factor that corresponds to path i and is the product of all reflection and transmission coefficients of the specific path, $\gamma(f)$ is the propagation constant of the electromagnetic wave at the utilized frequency f and d_i is the path's length.

The reflection and transmission coefficients, ρ and τ respectively, for a junction point of a distribution line, for a signal that is transmitted by device Tx towards Rx, are given by (2) and (3)

$$\rho = \frac{\left(Z_{0_{bi}} \| Z_{0_{bj}}\right) - Z_0}{\left(Z_{0_{bi}} \| Z_{0_{bj}}\right) + Z_0} \tag{2}$$

$$\tau = 1 + \rho \tag{3}$$

where $Z_{0_{bi}}$ and $Z_{0_{bj}}$ are the characteristic impedances of the transmission line segments that the signal is traveling towards and Z_0 corresponds to the characteristic impedance of the segment that carries the signal. Moreover, the reflection coefficient at a termination point can be calculated using (4)

$$\rho = \frac{Z_L - Z_0}{Z_L + Z_0} \tag{4}$$

where Z_L is the impedance of the termination.

For example, the reflection coefficient for a signal that travels towards junction A from device Tx, as shown in Fig. 3, is $\rho_{12} = ((Z_{0_3} \| Z_{0_5}) - Z_{0_2})/((Z_{0_3} \| Z_{0_5}) + Z_{0_2})$ and the respective transmission coefficient is $\tau_{32} = 1 + \rho_{12}$, where τ_{ij} and ρ_{ij} correspond to the transmission and reflection coefficient of a signal that passes from segment j to i respectively. In more detail, the multipath propagation that exists between two communication devices installed across a distribution network, as in Fig. 3 and the respective transfer functions of several paths are shown in Table I. The sum of the transfer functions of all possible paths equals to the total transfer function, but in the particular table some of the infinite paths are demonstrated.

In such a way, the lengths of all N directional segments of a network topology can be used for the calculation of the channel's transfer function adopting the procedure as it is explained in [24]. The particular method of transfer function calculation is adopted because its accuracy is validated through actual measurements, and it is easy to be implemented into a computer program. Furthermore, the main advantage that the specific method exhibits is the capability of computing the transfer function from one point to every other point existing in the studied topology including itself, by considering the transmitting and receiving device being installed in different directional segments.

After the derivation of the transfer function, this can be used to compute the channel's impulse response through the application of the inverse fast Fourier transform (IFFT).

$$H(f) \xrightarrow{IFFT} h(t) \tag{5}$$

The calculation of transfer function when the transmission and reception point is the same may seem meaningless in frequency domain, but it is treated only as a by-product of the procedure that aims to finally compute the impulse response in time domain through (5).

Moreover, when a HIF occurs across a rural distribution transmission line the topology of the network is changed. An additional impedance is present between two communication devices which affects the transfer function between the two points, as well as the impulse responses that can be measured from both ends simultaneously. A portion of a transmitted wave that travels over a transmission line section with a characteristic impedance Z_0 and reaches the point of a HIF, is reflected and the rest is transmitted with coefficients that are calculated using (6) and (7). If a topology containing N numbered directional segments is considered, an $N \times N$ matrix with all possible reflection and transmission coefficients may be formed, as explained in [24]. When a HIF occurs, the number of the topology's directional segments is changed to $N + 2$, and the dimension of the aforementioned matrix becomes $(N + 2) \times (N + 2)$. It has to be emphasized that this extra reflection point produces peaks in the impulse responses that were not present under normal operational conditions. This fact can easily be used to find the exact location of the fault, while the electromagnetic wave's propagation velocity is known for overhead transmission lines and assumed to be almost equal with the speed of light.

$$\rho_f = \frac{(Z_0 \| Z_f) - Z_0}{(Z_0 \| Z_f) + Z_0} \tag{6}$$

$$\tau_f = 1 + \rho_f \tag{7}$$

Observing (6) and (7), it may be easily deduced that if the fault impedance Z_f increases, the efficacy of the method decreases. As it was excepted, a HIF is impossible to be detected when its value is close to infinity, resulting to reflection coefficient close to zero and a transmission one close to unity. In mathematical terms this phenomenon is described by (8) and (9).

$$\lim_{Z_f \to \infty} \rho_f = \lim_{Z_f \to \infty} \frac{(Z_0 \| Z_f) - Z_0}{(Z_0 \| Z_f) + Z_0} = 0 \tag{8}$$

$$\lim_{Z_f \to \infty} \tau_f = \lim_{Z_f \to \infty} (1 + \rho_f) = 1 \tag{9}$$

Using the aforementioned method, the impulse response measured from both communication devices installed over a distribution line under no fault conditions can be calculated, knowing the topology of the network between them and the characteristics of the line, when an impulse is injected to the network from one of the devices. To that purpose, functions $h_{1n}(t)$ and $h_{2n}(t)$ may be introduced corresponding to the voltages measured from the two devices when an impulse is transmitted from one of them under normal operating conditions. Moreover, functions $h_{1f}(t)$ and $h_{2f}(t)$ may be also used representing respectively the voltages measured by the devices under the presence of a fault. In this case, the subtraction of these functions as shown in (10) may provide the necessary information for the extraction of the fault's location:

$$D(t) = h_{in}(t) - h_{if}(t) \tag{10}$$

where i is equal to the respective number identifying the examined communication device.

Furthermore, once a conductor is broken the topology among the two functioning devices will be entirely changed. At the point that a conductor is broken the electromagnetic wave is reflected with a coefficient equal to that of (4) with the only difference that instead of Z_L the high impedance value Z_f has to be added. The point has to be treated as a termination point rather than a junction one. The communication between transmitter and repeater is disrupted and the usage of the proposed method implementing specific impulse responses could easily provide the necessary information about the location of the fault, resulting to fast system restoration and, thus, beneficial outcome for both the utility and the public.

In both cases (i.e., of a HIF or a broken conductor), the fault distance from the impulse transmitting device, i, may be easily calculated. Applying a peak detection algorithm to both $h_{in}(t)$ and $D(t)$ matrices, vectors $\mathbf{P}_{in}$ and $\mathbf{P}_D$ may be created containing the time stamps of the occurring peaks of signals $h_{in}(t)$ and $D(t)$, respectively. By comparing these two vectors, the time stamp that corresponds to the fault location, t_f, is the minimum value of $\mathbf{P}_D$ that is not an element of $\mathbf{P}_{in}$. After identifying t_f, the distance of the fault from the impulse transmitting device, x_f, can be computed using (11):

$$x_f = \frac{\frac{2 \cdot \pi \cdot f}{\beta} \cdot t_f}{2} \tag{11}$$

where β corresponds to the imaginary part of the propagation constant γ, and $(2 \cdot \pi \cdot f)/\beta$ is equal to the speed of propagation, which is for overhead power lines almost equal to the speed of light. Finally, the fact that vector $D(t)$ has elements different from zero for both communication communication devices located before and after the fault, can be used for confirmation of the fault existence.

V. Detecting Fault Locations by the Use of Impulse Responses

For the evaluation of the proposed method which implements specific impulses for the acquisition of the fault's location an arbitrary distribution line segment is considered. This segment is located among two of the installed communication devices along the examined transmission line. To focus on the section where the HIF occurs, the points of the installed devices are considered to be matched, hence the effect of the rest of the network is ignored. Typical rural arrangements contain numerous branches. Therefore, the line segment under study may have from none to several branches, and its length is considered to be equal to the typical repeater span of a broadband PLC configuration, i.e., 1 km [9]–[12]. Moreover, the occurred fault will always be placed between two adjacent communication devices. These devices will be named device number 1 and device number 2. Specifically, device number 1 will be the device injecting the impulse into the network and measuring its reflections, while device number 2 will be the device receiving the injected impulse.

Furthermore, the electromagnetic wave characteristics of the transmission line, such as its characteristic impedance Z_0 and propagation constant γ are computed using D'Amore's *et al.*

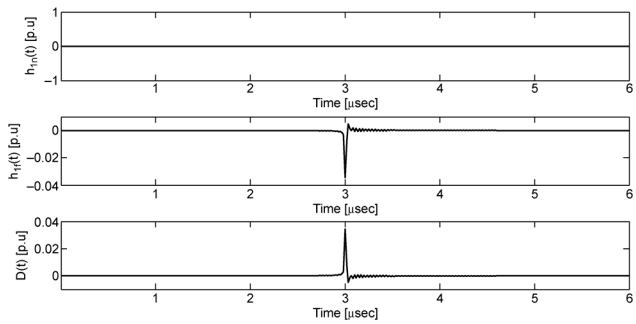

Fig. 4. Impulse responses of device number 1 at a 5 kΩ fault occurrence.

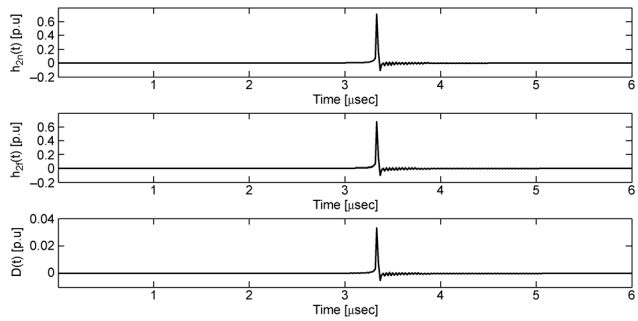

Fig. 5. Impulse responses of device number 2 at a 5 kΩ fault occurrence.

model [25], as shown in Part I. These quantities have to be calculated for a wide frequency range, because of the fact that the spectral content of an impulse is, as known, infinite in the frequency domain. Therefore, an upper frequency has to be set as a limit for the calculations of the channel's transfer function ensuring the validity of the outcome while taking into account the widest possible frequency range. This limit was set to be equal to the maximum frequency utilized by most PLC products, i.e., 30 MHz. Thus, the needed transfer functions are computed for a range that spreads from dc to 30 MHz, with a step equal to 50 Hz. Having computed the propagation constant for each contributing frequency the respective speed of propagation can be considered as *a priori* known. It can be derived that the majority of the used frequencies exhibit a speed of propagation that is really close to that of light. The frequencies that exhibit slower speed of propagation are responsible for the small time dispersion of the applied impulses. Therefore, it can be concluded that the impulses exhibit speed of propagation equal to that of light. Additionally, the magnitude of the impulses that are transmitted across the topology was considered to be equal to 1 V.

The first studied case corresponds to the occurrence of a HIF of 5 kΩ between two PLC devices that have to recognize and locate the fault. The topology between them contains no branches. The fault occurs 450 m away from the first device, which is device number 1. Once the existence of the fault is identified from the difference it creates to the overall arrangement's input impedance, as shown in Part I, the procedure of the injected impulses initiates. In Fig. 4 the voltage is shown as measured by device 1 after the injection of an impulse into the network from the same device, both under normal operation conditions, and when a fault exists, $h_{1n}(t)$ and $h_{1f}(t)$ respectively. Furthermore, the function $D(t)$ computed using (10) is plotted. The concept of the method lies into the fact that discontinuities of the characteristic impedance of the transmission line create additional points at which the waves will be reflected with a reflection coefficient computed using (6). Thus, extra peaks will appear at the impulse responses. Specifically, in Fig. 4 the function $h_{1n}(t)$ is equal to zero for the entire time period cause to the fact that the device 2 is considered to be matched and there is no branch between the two devices. On the other hand, observing function $h_{1f}(t)$ a peak is detected 3 μs after the injection which is created by the reflection on the HIF location. The speed of propagation is *a priori* known and almost equal to that of light, hence the exact fault location of 450 m away from device number 1 may easily be computed.

It should be noted that in practice the method results will naturally present some deviation, due to the corresponding small inaccuracy in the involved parameters. This holds for the above calculations, as well as for all calculations following in this work. However, this deviation is not expected to be significant as compared to the actual location results. As such, it is expected to have insignificant effect in practice, as the actual fault restoration will be performed by a man crew, which will need an approximate location in order to reach the fault quickly.

Moreover, in Fig. 5 the same quantities are plotted as they are recorded from device number 2 when an impulse is transmitted from device number 1. When a HIF is present between the two PLC devices, the electromagnetic waves are transmitted at the point of the fault with a corresponding transmission coefficient that is calculated using (7). Functions $h_{2n}(t)$ and $h_{2f}(t)$ have the same form, with a small divergence at their magnitudes, as shown by observing function $D(t)$. This difference exists due to the transmission coefficient τ_f and can also be used for the verification of the fault's occurrence.

Additionally, the occurrence of a larger HIF, with a value of 10 kΩ was studied, so as for the impact of the larger impedance to the method's efficacy to be investigated. The topology is considered to have one 100 m length open ended branch in the middle of the 1 km distance between the two PLC devices. The exact position of the HIF was selected to be equal to 450 m away from the first communication device. The HIF creates an extra node to the transmission line's arrangement, thus additional paths to the injected test signals. Its effect is presented in Fig. 6 and Fig. 7. The former shows the impulse response of the first device, whereas the latter the impulse response as it is measured from the second device. Specifically, in Fig. 6 the exact HIF location is detected through the first pulse that exists in $h_{1f}(t)$, 3 μs after the generation of the test signal while it is absent in $h_{1n}(t)$. Moreover, different pulses are recorded due to the extra paths that the fault inserts to the topology among the fault location, the point of the junction and the open end of the branch. By the observation of Fig. 7 divergences may be noticed for the same reason and, moreover, cause to the fact that the pulses are transmitted with a coefficient different from unity at the position of the fault. As it was expected, the reflection coefficient ρ_f is smaller as compared to the previous examined

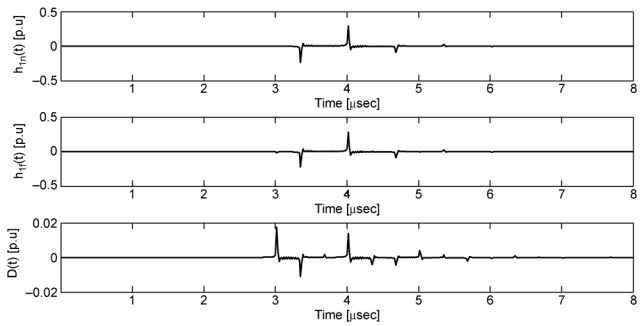

Fig. 6. Impulse responses of device number 1 at a 10 kΩ fault occurrence.

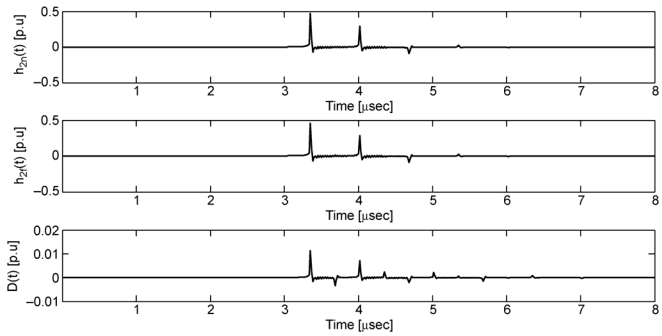

Fig. 7. Impulse responses of device number 2 at a 10 kΩ fault occurrence.

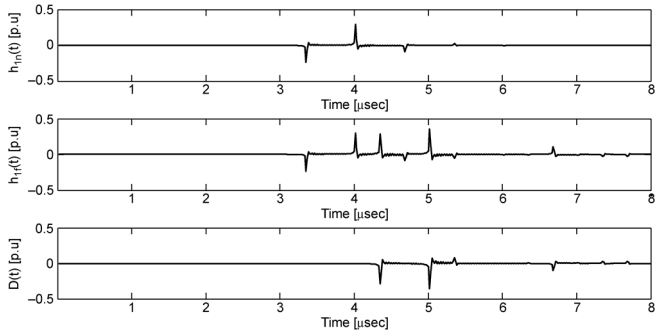

Fig. 8. Impulse responses of device number 1 at a broken conductor occurrence.

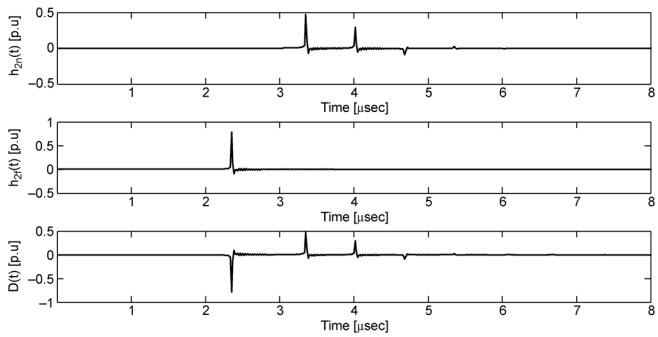

Fig. 9. Impulse responses of device number 2 at a broken conductor occurrence.

case. This results to additional generated pulses of lesser magnitude and the potential detection depends on the measurement sensitivity of the installed devices. When these magnitudes become smaller than the minimum value that the device can detect, the method becomes inapplicable. However, the sensitivity of the commercially available devices is deemed sufficient for the particular case study.

Another case of interest is the broken conductor one. The topology selected to be investigated in this case has one 100 m length open ended lateral branch at the middle of the 1 km distance between two PLC devices. The point at which the conductor is broken was selected to be equal to 650 m away from the first communication device. In Fig. 8 the responses as they are measured from the first device when it produces an impulse are illustrated. First, the impulse response under normal conditions is plotted and the multipath propagation inside the topology is easily observed. The first pulse that returns to the first device is the one reflected at the junction point 500 m away. Hence, it returns after having traversed twice this distance, after almost 3.33 μs. The other pulses are the products of the several reflections that occur between the junction point and the open end of the single branch and return to their point of origin. In the second subplot the impulse response after the conductor was broken at the predefined point is presented. It differs from the previous one at the times that pulses are reflected at the point of the fault, with the first reflection measured at 4.33 μs. This time can be easily attributed to the exact fault location. The rest of the measured peaks plotted in $D(t)$ are produced by the multipath propagation of the pulse reflected at the point of the fault. Furthermore, the communication between adjacent PLC devices is disrupted, and a special warning state can be declared. Afterwards, a test pulse can be injected by the other PLC device too for the verification of the calculated fault position. The results as they are recorded by this device are shown in Fig. 9. In this case, the pulse reaches the broken conductor point prior to the junction. Therefore, function $h_{2f}(t)$ has only one peak and that is the reflection of the test impulse to the open end that exists 350 m away from the device. In conclusion, the same fault location can be acquired and confirmed by both devices that are installed left and right of the occurred fault.

VI. Implementation of the Proposed Method in a Real Topology

The implementation of the proposed method requires information about the studied topology that can easily be acquired by the respective utility's geographical information system. This can be used for the calculation of the arrangement's input impedance under normal conditions for the chosen frequency range and the expected impulse responses between adjacent installed power line communication devices. Additionally, a specific combination of optimum frequencies that perform better than others may be determined, so that the total transmission line is monitored adequately. When a difference is detected in the input impedance value, a test signal injection procedure is initiated to locate the exact fault position.

For the presentation of a detailed theoretical application of the particular method, the topology that is part of the Greek rural distribution system examined in Part I of this work is considered. The lengths of all branches are known, and so are the terminations and the technical characteristics of the transmission line such as material, radius and height of conductors. The input impedance may be computed for the chosen frequency

TABLE II
DEVIATION AT OPTIMUM SELECTED FREQUENCIES FOR SEVERAL FAULT CASES

			Percentage input impedance divergences at chosen frequencies			
Fault type	Fault Impedance (kΩ)	Location (m)	f_1	f_2	f_3	f_4
HIF	1.5	12530	489.92	-63.09	66.85	2.19
HIF	5	3015	14.17	-39.06	35.07	39.97
HIF	7.5	2740	7.81	-31.43	20.24	26.19
HIF	10	4830	17.74	-13.98	29.12	6.43
Broken Conductor	-	4000	4223.2	-88.02	138.86	119.12

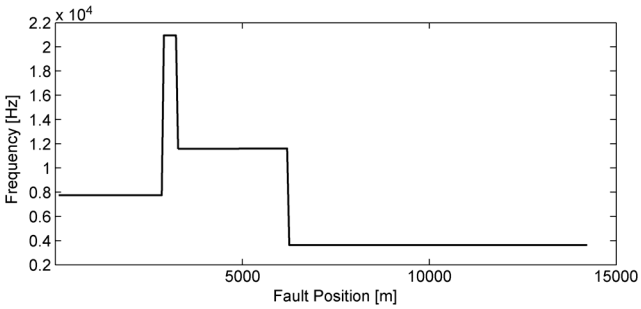

Fig. 10. Optimum frequencies for specific line's segments monitoring.

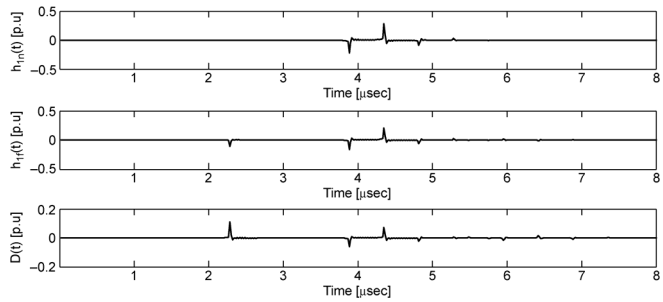

Fig. 11. Impulse responses of device number 1 at a 1.5 kΩ fault occurrence.

range, i.e., 3–95 kHz. Regarding several HIF at every point of the line the frequencies that perform best for specific segments may be extracted. These frequencies result from a theoretical methodology, in which different fault impedance values are tested versus all possible fault locations for the determination of the frequencies with the best performance, i.e., the highest percentage deviation. From the rigorous investigation of the calculations, four frequencies are selected to monitor the total length of the specific topology. The chosen frequencies, and the corresponding line segments that are monitored satisfactorily by them are presented in Fig. 10. Specifically, it is shown that frequency f_1 that is equal to 3635 Hz exhibits best for more than the half of transmission line's length. Additionally, frequencies f_2, f_3, f_4 which are equal to 7730, 11 590, and 20 955 Hz respectively, may be used to monitor the rest of the topology. In Table II, several HIF cases, a broken conductor one, as well as the percentage divergence recorded for the overall input impedance for each case are presented. It can be deduced that, as it is shown in Fig. 10, there is one optimum frequency for every fault location. For example, for the 5 kΩ HIF that occurs 3015 meters away from the topology's starting point, the best performing frequency is the f_4. The same information is deduced from Table II too. Furthermore, for every examined case the divergences for at least one of the selected frequencies are significant and this can lead to effective detection.

If the first case of Table II is considered, when the fault occurs and the divergences at the input impedance are measured, the impulse response procedure has to start. Thus the respective installed PLC devices inject a test pulse into the network, and through the comparison between what is measured and the impulse response under normal conditions, the exact fault location is determined. Moreover, considering that the closest PLC devices to the fault's location are installed 12 190 m and 13 190 m away from the arrangement's starting point, only the impulse responses of those two devices are studied. The examined topology between the devices contains a junction point 580 m away from device number 1, from which starts a 70 m lateral branch that ends up to an open termination. The distance between the devices is again 1 km, i.e., equal to the typical PLC repeater span. The impulse responses recorded by both devices when device number 1 generates a test impulse are shown in Fig. 11 and Fig. 12, respectively. Observing the responses when the fault occurs, and comparing them with those that correspond to normal operational conditions, additional peaks are detected, which are products of the extra paths created due to the fault presence. Specifically, in $h_{1f}(t)$ of Fig. 11, the first peak is recorded 2.26 μs after the injection that is considered to happen at the time instant $t = 0$. Moreover, peaks that are not present at the plot of $h_{1n}(t)$, and are generated because of the reflections occurring among all points of discontinuity in the characteristic impedance are detected. Finally, it is observed that the peaks recorded at exact the same moments before and after the fault occurrence, differ in magnitude. This may also be used for the effective detection. Similar conclusions are taken from Fig. 12. Using a simple peak detection algorithm and the known propagation speed of the impulse, the location of the fault, which is 340 m away from device number 1, can be derived.

VII. CONCLUSION

In the present work a complete method for the detection and location of high impedance faults (HIFs) in a smart grid is presented. In Part I the influence of a HIF presence on the arrangement's overall input impedance for a chosen frequency range, that extends from 3 to 95 kHz, is thoroughly explained. It is deduced that a small number of frequencies may be used to monitor the entire length of the transmission line satisfactorily. A

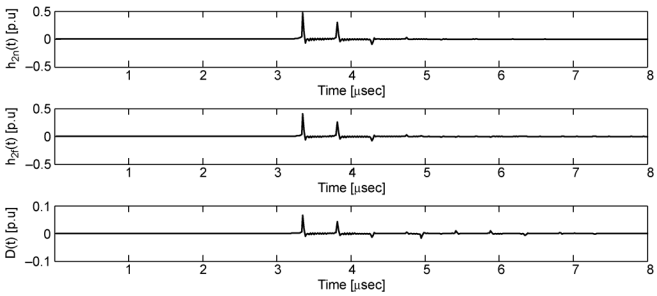

Fig. 12. Impulse responses of device number 2 at a 1.5 kΩ fault occurrence.

change to the topology's input impedance at the chosen frequencies could indicate a HIF occurrence.

This part of the study can be combined with the usage of installed PLC devices along the distribution line's length to locate the exact position of the fault. These devices, which are originally installed for the transmission of important information for the operation of the smart grid, may also be utilized for the aforementioned purpose by injecting specific test impulses into the network. It is shown that, by the comparison of the recorded impulse responses under normal operational conditions and under a fault presence, additional peaks are observed. These peaks are due to the extra point of discontinuity in the transmission line characteristic impedance, thus due to the extra paths that the topology contains after the fault occurrence. Moreover, the impulse responses that the communication devices closest to the fault measure are different from those that correspond to the case that no fault occurs. By applying a simple peak detection algorithm and using the known propagation speed of the pulse the exact HIF location can be derived with high accuracy.

ACKNOWLEDGMENT

The authors would like to thank Mrs. S. Fahouridis and A. Zafirakis of the Public Power Corporation (PPC) of Greece for providing the needed data that enabled this study to be conducted successfully.

REFERENCES

[1] D. Ibrahim, T. El Sayed, E.-D. El-Zahab, and S. Saleh, "Unsynchronized fault-location scheme for nonlinear hif in transmission lines," *IEEE Trans. Power Del.*, vol. 25, no. 2, pp. 631–637, April 2010.

[2] A. Borghetti, M. Bosetti, M. Di Silvestro, C. Nucci, and M. Paolone, "Continuous-wavelet transform for fault location in distribution power networks: Definition of mother wavelets inferred from fault originated transients," *IEEE Trans. Power Syst.*, vol. 23, no. 2, pp. 380–388, May 2008.

[3] A. Borghetti, M. Bosetti, C. Nucci, M. Paolone, and A. Abur, "Integrated use of time-frequency wavelet decompositions for fault location in distribution networks: Theory and experimental validation," *IEEE Trans. Power Del.*, vol. 25, no. 4, pp. 3139–3146, Oct. 2010.

[4] A. Bretas, M. Moreto, R. Salim, and L. Pires, "A novel high impedance fault location for distribution systems considering distributed generation," in *Proc. IEEE/PES Transm. Distrib. Conf. Expo.: Latin America (TDC)*, Aug. 2006, pp. 1–6.

[5] M. Kezunovic, "Smart fault location for smart grids," *IEEE Trans. Smart Grid*, vol. 2, no. 1, pp. 11–22, Mar. 2011.

[6] Y.-S. Ko, "A self-isolation method for the hif zone under the network-based distribution system," *IEEE Trans. Power Del.*, vol. 24, no. 2, pp. 884–891, Apr. 2009.

[7] N. Sarma, V. Prasad, K. Prakasa Rao, and V. Sankar, "A new network reconfiguration technique for service restoration in distribution networks," *IEEE Trans. Power Del.*, vol. 9, no. 4, pp. 1936–1942, Oct. 1994.

[8] S. Galli, A. Scaglione, and Z. Wang, "For the grid and through the grid: The role of power line communications in the smart grid," *Proc. IEEE*, vol. 99, no. 6, pp. 998–1027, Jun. 2011.

[9] P. Amirshahi and M. Kavehrad, "High-frequency characteristics of overhead multiconductor power lines for broadband communications," *IEEE J. Sel. Areas Commun.*, vol. 24, no. 7, pp. 1292–1303, Jul. 2006.

[10] P. Amirshahi and M. Kavehrad, "Medium voltage overhead power-line broadband communications; Transmission capacity and electromagnetic interference," in *Proc. Int. Symp. Power Line Commun. Its Appl.*, Apr. 2005, pp. 2–6.

[11] A. Lazaropoulos and P. Cottis, "Transmission characteristics of overhead medium-voltage power-line communication channels," *IEEE Trans. Power Del.*, vol. 24, no. 3, pp. 1164–1173, Jul. 2009.

[12] A. Lazaropoulos and P. Cottis, "Capacity of overhead medium voltage power line communication channels," *IEEE Trans. Power Del.*, vol. 25, no. 2, pp. 723–733, Apr. 2010.

[13] J. Anatory, N. Theethayi, R. Thottappillil, M. Kissaka, and N. Mvungi, "Broadband power-line communications: The channel capacity analysis," *IEEE Trans. Power Del.*, vol. 23, no. 1, pp. 164–170, Jan. 2008.

[14] D. Spoor and J. G. Zhu, "Improved single-ended traveling-wave fault-location algorithm based on experience with conventional substation transducers," *IEEE Trans. Power Del.*, vol. 21, no. 3, pp. 1714–1720, Jul. 2006.

[15] G. Ancell and N. Pahalawaththa, "Maximum likelihood estimation of fault location on transmission lines using travelling waves," *IEEE Trans. Power Del.*, vol. 9, no. 2, pp. 680–689, Apr. 1994.

[16] P. Varaiya, F. Wu, and J. Bialek, "Smart operation of smart grid: Risk-limiting dispatch," *Proc. IEEE*, vol. 99, no. 1, pp. 40–57, Jan. 2011.

[17] R. Lasseter, "Smart distribution: Coupled microgrids," *Proc. IEEE*, vol. 99, no. 6, pp. 1074–1082, Jun. 2011.

[18] Y. Yu and W. Luan, "Smart grid and its implementations," *Proc. Chinese Soc. Electr. Eng.*, vol. 29, no. 34, pp. 1–8, 2009.

[19] X. Q. Q. Lu and G. He, "Smart grid and smart wide area robot," *Proc. Chinese Soc. Electr. Eng.*, vol. 31, no. 34, pp. 1–5, 2011.

[20] E. Commission *et al.*, "Strategic research agenda for Europe's electricity networks of the future," 2007.

[21] H. Farhangi, "The path of the smart grid," *IEEE Power Energy Mag.*, vol. 8, no. 1, pp. 18–28, Jan.–Feb. 2010.

[22] B. Russell and C. Benner, "Intelligent systems for improved reliability and failure diagnosis in distribution systems," *IEEE Trans. Smart Grid*, vol. 1, no. 1, pp. 48–56, Jun. 2010.

[23] A. Meliopoulos, G. Cokkinides, R. Huang, E. Farantatos, S. Choi, Y. Lee, and X. Yu, "Smart grid technologies for autonomous operation and control," *IEEE Trans. Smart Grid*, vol. 2, no. 1, pp. 1–10, Mar. 2011.

[24] X. Ding and J. Meng, "Channel estimation and simulation of an indoor power-line network via a recursive time-domain solution," *IEEE Trans. Power Del.*, vol. 24, no. 1, pp. 144–152, Jan. 2009.

[25] M. D'Amore and M. Sarto, "Simulation models of a dissipative transmission line above a lossy ground for a wide-frequency range. i. single conductor configuration," *IEEE Trans. Electromagn. Compat.*, vol. 38, no. 2, pp. 127–138, May 1996.

Apostolos N. Milioudis was born in Xanthi, Greece, on February 27, 1985. He received the Dipl.-Eng. degree from the Department of Electrical and Computer Engineering at the Aristotle University of Thessaloniki, Greece, in 2007. He is currently working toward the Ph.D. degree at the same university.

His special interests are power system analysis with special emphasis on the simulation of transmission and distribution systems, high impedance fault detection techniques, artificial intelligence applications in power systems, and power line communications.

Georgios T. Andreou (S'98–A'02–M'08) was born in Thessaloniki, Greece, on August 16, 1976. He received the Dipl.-Eng. and Ph.D. degrees from the Department of Electrical and Computer Engineering at the Aristotle University of Thessaloniki in 2000 and 2006, respectively.

Currently he is a Lecturer at the same Department. His special interests are power system analysis with special emphasis on the simulation of transmission and distribution systems, electromagnetic and thermal field analysis, and power line communications.

Dimitrios D. Labridis (S'88–M'90–SM'00) was born in Thessaloniki, Greece, on July 26, 1958. He received the Dipl.-Eng. and the Ph.D. degrees from the Department of Electrical and Computer Engineering, Aristotle University of Thessaloniki, Greece, in 1981 and 1989, respectively.

Since 1990 he has been with the Electrical Engineering Department, Aristotle University of Thessaloniki, where he is currently a Professor. His research interests are power system analysis with special emphasis on the simulation of transmission and distribution systems.